International Journal of Advanced and Applied Sciences, 10(2) 2023, Pages: 166-174

Contents lists available at Science-Gate

International Journal of Advanced and Applied Sciences

Journal homepage: http://www.science-gate.com/IJAAS.html

Numerical solution for MHD flow and heat transfer of Maxwell fluid over a stretching sheet

Faisal Salah *, A. Alqarni

Department of Mathematics, College of Science and Arts, King Abdul-Aziz University, Jeddah, Saudi Arabia

ARTICLE INFO

Article history:
Received 12 July 2022
Received in revised form
24 October 2022
Accepted 7 November 2022

Keywords:
Maxwell fluid
Successive linearization
Heat transfer
MHD
Stretching sheet channel

ABSTRACT

In this article, the numerical solutions for the flow of heat transfer for an incompressible Maxwell fluid on a stretching sheet channel are presented in this study. By applying appropriate transformations, the system of governing partial differential equations is transformed into a system of ordinary differential equations. A successive linearization method (SLM) is used to describe and solve the resulting nonlinear equations numerically using MATLAB software. The main goal of this paper is to compare the results of solving the velocity and temperature equations in the presence of β_1 changes through SLM for introducing it as a precise and appropriate method for solving nonlinear differential equations. Tables with the numerical results are created for comparison. This contrast is important because it shows how precisely the successive linearization method can resolve a set of nonlinear differential equations. Non-Newtonian parameters on the flow field, like mixed convection, Hartman, Deborah, and Prandtl numbers, are explored and illustrated graphically. Apart from that, a great deal of agreement has been seen between the current results and the published data that have been evaluated and compared in a limited way.

1. Introduction

Engineering and industrial processes like extrusion processes, biological fluid flow, hot rolling, glass-fiber production, cooling of metallic plates, rubber sheets, lubricant and paint performance, wire drawing, melt-spinning, plastic manufacturing, the extrusion of polymers, and aerodynamic plastic sheet extrusion, among others, are required and have attracted significant attention in recent decades to study flow on a stretching sheet. The movement of fluid over a stretched surface is being studied by several scholars (Reddy et al., 2021). Nonlinear behavior is one of the most common occurrences in engineering and research. The equations become more complex to handle and solve as a result of the nonlinearity. Approximate analytical approaches, such as the Homotopy analysis method (HAM) (Liao, 1992; 2004), can be used to solve some of these nonlinear equations. The Homotopy Perturbation method (HPM) was found by He (1999) and the Adomain decomposition method (ADM) (Esmaili et al., 2008; Makinde and Mhone, 2006; Makinde, 2008). However, some of these equations are solved via traditional numerical techniques such as the finite difference method, shooting method and Keller box method, Runge-Kutta, and artificial neural networks (ANNs) (Shateyi and Motsa, 2010; Shafiq et al., 2021). The governing equation for the Maxwell fluid is of fourth order in general. When higher-order nonlinearities are neglected, the order of the equation in the Maxwell fluid is reduced. Recently some studies have presented a new method called Successive Linearization Method (SLM). This method has been applied successfully in many nonlinear problems in sciences and engineering, such as the MHD flows of non-Newtonian fluids and heat transfer over a stretching sheet (Shafiq et al., 2022), viscoelastic squeezing flow between two parallel plates, (Makukula et al., 2010a), two-dimensional laminar flow between two moving porous walls (Makukula et al., 2010b) and convective heat transfer for MHD boundary layer with pressure gradient (Ahmed et al., 2015), the thin-film flow of Eyring-Powell fluid on the vertically moving belt (Salah et al., 2019). Therefore, the effectiveness, validity, accuracy, and flexibility of the SLM are verified among all these successful applications.

Fluid applications have gotten a lot of attention in the last several years. Some fluids, unlike viscous

* Corresponding Author.
Email Address: faisal19999@yahoo.com (F. Salah)
https://doi.org/10.21833/ijaas.2023.02.020
Corresponding author's ORCID profile:
https://orcid.org/0000-0003-0410-001X

fluids, have a difficult time expressing themselves through a specific constitutive relationship between shear rates and stress (Ellahi et al., 2008; Hayat et al., 2004). These fluids, which include a variety of household things such as toiletries, paints, cosmetics, some oils, shampoo, jams, soups, and so on, have distinct characteristics and are designated as non-Newtonian fluids. Non-Newtonian fluid models are classified into three categories: integral, differential, and rate types (Fetecau et al., 2007; Salah et al., 2011a; 2011b). In the present study, the main interest is to discuss the heat transfer flow of magnetohydrodynamic (MHD) Maxwell fluid over a stretching sheet. The effects of the stretching sheet on fluid flow have piqued the interest of a number of scientists, resulting in a substantial amount of research. Shaping is the most significant industry for improving the output and ductility of precise pieces. Extrusion casting, drawing, plastic films, polymer, hot rolling, and other engineering applications can all benefit from the study of MHD fluid flow on stretching sheets. Researchers in this discipline are constantly trying to enhance accuracy by employing various methodologies on fluid behavior in order to keep up with breakthroughs in the field. The application of magnetohydrodynamic flow was one of the techniques used in this sector (Ghadikolaei et al., 2018). This application is known as MHD. The study of the interaction of electrically conductive fluids with electromagnetic events is known as MHD. In many areas of applied science, engineering, and technology, such as MHD pumps and MHD power production, the flow of MHD fluid in the presence of a magnetic field is critical. As a result, numerous researchers continue to contribute to the field of MHD fluid mechanics (Hayat et al., 2013; Malik et al., 2013; Hussain et al., 2010; Husain et al., 2008). Another important application of nanoparticles in the base fluid is seeking to improve the behavior of fluid and madding optimal use of the changes. Due to various engineering issues and different boundary conditions, intensive research has been achieved in this field, which is summarized briefly. Because of various boundary conditions and different engineering situations, Waqas et al. (2017) discussed the stratified flow of nonliquid with heat generation in a linear stretchable surface. Ghadikolaei et al. (2018) analyzed the flow and heat transfer of second-grade fluid on a stretching sheet channel. The study of heat transfer with mixed convection flow of nonliquid that passed through a stretching perpendicular plate with the presence of three various types of nanoparticles, Cu, Al_2O_3, and TiO_2 to analyze various thermal conductivity of the nonliquid and the velocity of nanoparticles and the research on the Nusselt number was found out by Si et al. (2017). There are many available published works in this field (Zargartalebi et al., 2015; Megahed, 2013; Sadeghy et al., 2006; Mukhopadhyay 2012; Subhas Abel et al., 2012; Cortell, 2006). Wang et al. (2022) discussed the Natural bio-convective flow of Maxwell Nanofluid over an exponentially stretching surface with slip effect and convective boundary condition and they conclude that by the enhancement of the magnetic characteristic and Deborah number, the fluid velocity is declining due to occurrence of retardation effect (Wang et al., 2022). Many attempts have been made for Maxwell fluid over an exponentially stretching surface (Aman et al., 2017; Aman et al., 2020; Xu et al., 2021; Abdal et al., 2022; Saleem et al., 2020; Aman and Almdallal, 2019). Presently a new investigation on heat transfer of an incompressible Maxwell fluid on a stretching sheet channel is discussed. The governing equations of Maxwell fluid with MHD are utilized. The numerical solution to the resulting nonlinear problem is computed by using the SLM approach. The embedded flow parameters are discussed and illustrated graphically.

2. Description of the mathematical model

2.1. Flow analysis

Here we consider two–dimensional steady laminar flow of an incompressible MHD Maxwell fluid, which is past a flat sheet that coincides with the plane $y = 0$. Then the flow is confined to the section $y > 0$. Along x- axis there are two opposite and equal forces applied. Due to this, the wall is reserved and stretching the origin fixed (Fig. 1).

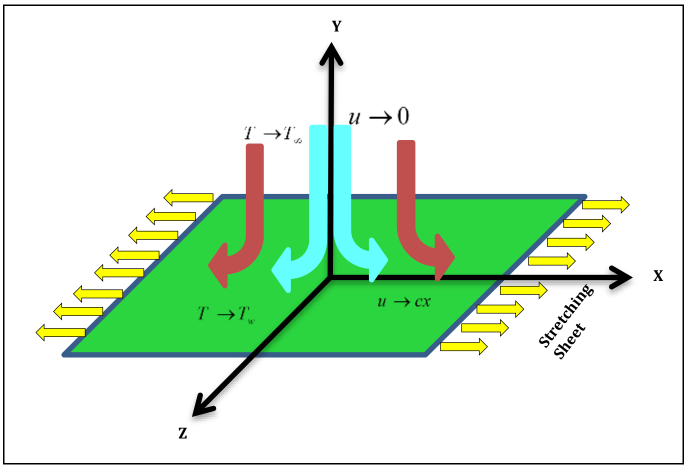

Fig. 1: Geometry of the problem

Under the constant and boundary layer assumptions, the continuity, constitutive equation of Maxwell fluid and energy equation are Subhas Abel et al. (2012) and Ghadikolaei et al. (2018):

$$\frac{\partial u}{\partial x}+\frac{\partial v}{\partial y}=0 \quad (1)$$

$$u\frac{\partial u}{\partial x}+v\frac{\partial u}{\partial y}+\beta\left(u^2\frac{\partial^2 u}{\partial x^2}+v^2\frac{\partial^2 u}{\partial y^2}+2uv\frac{\partial^2 u}{\partial x\partial y}\right)=v\frac{\partial^2 u}{\partial y^2}-\frac{\sigma B_0^2}{\rho}\left(u+\beta v\frac{\partial u}{\partial y}\right)+g\beta_T(T-T_\infty) \quad (2)$$

$$u\frac{\partial T}{\partial x}+v\frac{\partial T}{\partial y}=\alpha\frac{\partial^2 T}{\partial y^2}+\frac{k}{c_p}\left(\frac{\partial u}{\partial y}\right)^2 \quad (3)$$

where, (u,v) denote the components of velocity in (x,y) directions, $v\left(=\frac{\mu}{\rho}\right)$the kinematic viscosity, μ is the dynamic viscosity, β is the relaxation time, ρ density of the fluid, σ is the electric conductivity, B_0 is the uniform magnetic fluid, g is the gravitational acceleration, β_T the coefficient of thermal expansion, T is the temperature of the fluid, $\alpha\left(=\frac{k}{\rho c}\right)$ the thermal diffusivity, k the fluid thermal conductivity, ρc the fluid capacity heat and c_p the specific heat.

The relevant boundary conditions are defined by Cortell (2006):

$$u=u_w=cx, v=0 \text{ at } y=0, c>0 \quad (4)$$

$$u\to 0, \frac{\partial u}{\partial y}\to 0 \text{ as } y\to\infty, \quad (5)$$

$$T=T_w(=T_\infty+Ax^s) \text{ at } y=0, \quad T\to T_\infty \text{ as } y\to\infty. \quad (6)$$

where, c the stretching is rate, T_w and $T_\infty$are constants and s is the parameter of wall temperature.

2.2. Transformation

Introducing the following dimensionless variables:

$$u=cxf'(\eta), v=-(cv)^{\frac{1}{2}}f(\eta), \eta=\left(\frac{c}{v}\right)^{\frac{1}{2}}y, \theta(\eta)=\frac{T-T_\infty}{T_w-T_\infty}, Ec=\left(\frac{c^2}{Acp}\right). \quad (7)$$

Utilizing Eq. 7, Eq. 1 is satisfied automatically and Eqs. 2 and 3 characterize the following problems statement:

$$f'''+ff''-f'^2+\beta_1(2ff'f''-f^2f''')-M^2f'+\lambda\theta=0 \quad (8)$$

$$\theta''+\mathrm{Pr}f\theta'-s\mathrm{Pr}f'\theta=-\mathrm{Pr}Ec(f'')^2 \quad (9)$$

Clearly that all solutions for Eq. 9 are in similar type when $s=2$. If we neglected the dissipative heat, then Eq. 9 takes the simpler form:

$$\theta''+\mathrm{Pr}f\theta'-2\mathrm{Pr}f'\theta=0 \quad (10)$$

Here $\beta_1(=\beta c)$ the Deborah number, $M\left(=\sqrt{\frac{\sigma B_0^2}{c\rho}}\right)$ is the Hartman number, $\lambda\left(=\frac{Gr_x}{\mathrm{Re}_x^2}\right)$ is the mixed convection parameter, $\mathrm{Pr}\left(=\frac{v}{\alpha}\right)$ is the Prandtl number and $Ec\left(=\frac{c^2}{Acp}\right)$ is the Eckert number.

The related boundary conditions:

$$f=0, f'=1 \quad at \quad \eta=0, \quad (11)$$

$$f'\to 0, f''\to 0 \quad as \quad \eta\to\infty. \quad (12)$$

$$\theta(0)=1, \quad \theta(\infty)\to 0. \quad (13)$$

3. Solution the problem

3.1. Procedure of computational

Here successive linearization method (SLM) (Makukula et al., 2010a; 2010b; Ahmed et al., 2015; Salah et al., 2019) is implemented to obtain the numerical solutions for nonlinear systems 8 and 10 corresponding to the boundary condition Eqs. 11–13.

For the SLM solution, we select the initial guess functions $f(\eta)$ and $\theta(\eta)$ in the form:

$$f(\eta)=f_i(\eta)+\sum_{m=0}^{i-1}F_m(\eta), \qquad \theta(\eta)=\theta_i(\eta)+\sum_{m=0}^{i-1}\theta_m(\eta). \quad (14)$$

Here the two functions $f_i(\eta)$ and $\theta_i(\eta)$ are representative of unknown functions. $F_m(\eta), m\geq 1$, $\theta_m(\eta), m\geq 1$ are successive approximations that are obtained by recursively solving the linear part of the equation that results from substituting Eq. 14 in Eqs. 8 and 9.

The strategy of SLM is the assumption of an unknown function $f_i(\eta)$ and $\theta_i(\eta)$ are smaller when i becomes very large, therefore, the nonlinear terms in $f_i(\eta)$, $\theta_i(\eta)$ and their derivatives are considered to be smaller and thus neglected. The intimal guess functions $F_o(\eta)$, $\theta_o(\eta)$ which are selected to satisfy the boundary conditions:

$$F_0(\eta)=0, F'_0(\eta)=1 \quad at \quad \eta=0,$$

$$F'_0(\eta)\to 0, \; F''_0(\eta)\to 0 \quad at \quad \eta\to\infty,$$

$$\theta_o(0)=1, \theta_o(\infty)\to 0. \quad (15)$$

which are taken to be in the form:

$$F_0(\eta)=(1-e^{-\eta}) \text{ and } \theta_0(\eta)=e^{-\eta}. \quad (16)$$

Therefore, beginning from the initial guess, the subsequent solution F_i and θ_i are calculated by successively solving the linearized from the equation which is obtained by substituting Eq. 14 in Eqs. 8 and 10. Then we get the linearized equations:

$$a_{1,i-1}F_i'''+a_{2,i-1}F_i''+a_{3,i-1}F_i'+a_{4,i-1}F_i+\lambda\theta_i=r_{1,i-1} \quad (17)$$

$$b_{1,i-1}F_i'+b_{2,i-1}F_i+\theta_i''+b_{3,i-1}\theta_i'+b_{4,i-1}\theta_i=r_{2,i-1} \quad (18)$$

Subject to the boundary conditions:

$$F_i(0)=\theta_i(\infty)=0, F'_i(0)=\theta_i(0)=1 \quad (19)$$

where, the coefficients parameters $a_{k,i-1}, b_{k,i-1}(k=1,2,3,4)$ and $r_{j,i-1}, j=1,2$ are defined as:

$a_{1,i-1} = 1 - \beta_1\left(\sum_{m=0}^{i-1} F_m\right)^2, a_{2,i-1} = \sum_{m=0}^{i-1} F_m + 2\beta_1 \sum_{m=0}^{i-1} F_m \sum_{m=0}^{i-1} F'_m,$

$a_{3,i-1} = -2\sum_{m=0}^{i-1} F'_m - M^2 + 2\beta_1 \sum_{m=0}^{i-1} F_m \sum_{m=0}^{i-1} F''_m\,,$

$a_{4,i-1} = \sum_{m=0}^{i-1} F''_m + 2\beta_1 \sum_{m=0}^{i-1} F_m \sum_{m=0}^{i-1} F''_m - 2\beta_1 \sum_{m=0}^{i-1} F_m \sum_{m=0}^{i-1} F_m''',$

and

$$r_{1,i-1} = -\sum_{m=0}^{i-1} F_m''' - \sum_{m=0}^{i-1} F_m \sum_{m=0}^{i-1} F''_m + \left(\sum_{m=0}^{i-1} F'_m\right)^2 - \beta_1\left[2\sum_{m=0}^{i-1} F_m \sum_{m=0}^{i-1} F'_m \sum_{m=0}^{i-1} F''_m - \left(\sum_{m=0}^{i-1} F_m\right)^2 \sum_{m=0}^{i-1} F_m'''\right] + M^2 \sum_{m=0}^{i-1} F'_m - \lambda \sum_{m=0}^{i-1} \theta_m \quad (20)$$

$b_{1,i-1} = -2\mathrm{Pr}\sum_{m=0}^{i-1} \theta_m\,,\; b_{2,i-1} = \mathrm{Pr}\sum_{m=0}^{i-1} \theta'_m,\; b_{3,i-1} = \mathrm{Pr}\sum_{m=0}^{i-1} F_m,\; b_{4,i-1} = -2\mathrm{Pr}\sum_{m=0}^{i-1} F'_m$

$$r_{2,i-1} = -\sum_{m=0}^{i-1} \theta''_m - \mathrm{Pr}\sum_{m=0}^{i-1} F_m \sum_{m=0}^{i-1} \theta'_m + \mathrm{Pr}\sum_{m=0}^{i-1} F'_m \sum_{m=0}^{i-1} \theta_m. \quad (21)$$

When we solve Eqs. 8 and 10 iteratively, the solution for F_i and θ_i has been obtained and finally after K iterations the solution $f(\eta)$ and $\theta(\eta)$ can be written as $f(\eta) \approx \sum_{m=0}^{K} F_m(\eta), \theta(\eta) \approx \sum_{m=0}^{K} \theta_m(\eta)$. In order to apply SLM, initially we transform the domain solution from $[0,\infty)$ to $[-1,1]$. SLM is dependent on the Chebyshev spectral collection method.

This method is depending on the Chebyshev polynomials defined on the interval $[-1,1]$. Thus, by using the truncation of domain approach where the problem is solved in the interval $[0, L]$ where L denotes the scaling parameter which is used to impose the boundary condition at infinity. Thus, this can be obtained via the transformation:

$$\frac{\eta}{L} = \frac{\xi+1}{2}, -1 \le \xi \le 1. \quad (22)$$

By using the Gauss-Lobatto collocation points we can discretize the domain $[-1,1]$ as follows:

$$\xi = \cos\frac{\pi j}{N}, F_i \approx \sum_{k=0}^{N} F_i(\xi_k) T(\xi_j), j = 0,1,\dots N \quad (23)$$

where, N is the number of collection points and T_k is the k^{th} Chebyshev polynomial is given by $T_k(\xi) = \cos[k\cos^{-1}(\xi)]$.

The derivatives of the variable at the collocation points are in the form:

$$\frac{d^r F_i}{d\eta^r} = \sum_{k=0}^{N} D_{kj}^r F_i(\xi_k), j = 0,1,\dots N$$

$$\frac{d^r \theta_i}{d\eta^r} = \sum_{k=0}^{N} D_{kj}^r \theta_i(\xi_k), j = 0,1,\dots N \quad (24)$$

where r is denote the order of differentiation and $\boldsymbol{D} = \frac{2}{L}\boldsymbol{D}$ with $\boldsymbol{D}$ is the Chebyshev spectral differentiation matrix. Substituting Eqs. 22 to 24 into Eqs. 17 and 18 we arrive at the matrix equation:

$$\boldsymbol{A}_{i-1}\boldsymbol{X}_i = \boldsymbol{R}_{i-1} \quad (25)$$

$$\boldsymbol{A}_{i-1} = \begin{bmatrix} A_{11} & A_{12} \\ A_{21} & A_{22} \end{bmatrix}, \; \boldsymbol{x}_{i-1} = \begin{bmatrix} \boldsymbol{F}_i \\ \boldsymbol{\theta}_i \end{bmatrix}, \; \boldsymbol{R}_{i-1} = \begin{bmatrix} r_{1,i-1} \\ r_{2,i-1} \end{bmatrix}$$

where,

$\boldsymbol{A_{11} = a_{1,i-1}D^3 + a_{2,i-1}D^2 + a_{3,i-1}D + a_{4,i-1}I,}$
$\boldsymbol{A_{12} = \lambda I,}$
$\boldsymbol{A_{21} = b_{1,i-1}D + b_{2,i-1}I,}$
$\boldsymbol{A_{22} = D^2 + b_{3,i-1}D + b_{4,i-1}I.}$

Following the above procedure, we can obtain the solution:

$$\boldsymbol{X_i = A^{-1}R_{i-1}}. \quad (26)$$

3.2. Convergence analysis

Table 1 illustrates the convergence for the numerical values of the skin friction coefficient and the local Nusselt number.

Table 1: The convergence for numerical values of $-f''(0)$ for different order of approximation when $M = 0.50, \beta_1 = 0.26, \mathrm{Pr} = 0.48$ and $\lambda = 0.43$

Order of approximation	$-f''(0)$	$-\theta'(0)$
1	0.9776756524	0.8369450287
5	0.9612200665	0.8481192201
10	0.9529250443	0.8518377291
20	0.9476560827	0.8532002153
30	0.9472383897	0.8532702100
50	0.9472212121	0.8532722292
70	0.9472212200	0.8532722263
75	0.9472212201	0.8532722263
80	0.9472212201	0.8532722263
90	0.9472212201	0.8532722263
100	0.9472212201	0.8532722263

3.3. Numerical scheme testing

Here, we test the validity of our numerical results and contrast them with those of published works as limiting examples. Thus, we compare the present results with the available results such as Waqas et al. (2017), Megahed (2013), Mukhopadhyay (2012), and Subhas Abel et al. (2012); it is found that our results are excellent agreement as shown in Table 2.

Table 2: Comparison of numerical values of $-f''(0)$ with other works for several values of β_1 when $M = 0 = \lambda = \mathrm{Pr}$

β_1	Waqas et al. (2017)	Megahed (2013)	Mukhopadhyay (2012)	Subhas Abel et al. (2012)	Present work
0.0	1.000000	0.999978	0.9999963	1.00000	0.999999
0.2	1.051889	1.051945	1.051949	1.05194	1.051889
0.4	1.101903	1.101848	1.101851	1.10184	1.101903
0.6	1.150137	1.150163	1.150162	1.15016	1.150137
0.8	1.196711	1.196690	1.196693	1.19872	1.196711
1.0	-	-	-	-	1.241747

4. Results and discussion

The successive linearization method was used to construct the graphical representations of velocity and temperature profiles in this section. These graphs illustrate the variations in embedded flow parameters for incompressible MHD Maxwell fluid flows over a stretching sheet channel. The physical understanding of the issue is examined in Figs. 2–9.

These data points are shown to show these changes. Here the graphs have been determined for the MHD heat transfer flow of steady Maxwell fluid over a stretching sheet. Fig. 2 is prepared to show the role of Hartman number M on the velocity field profile. By fixing $\beta_1, \mathrm{Pr}, \lambda$ and varying M, it is notice that the velocity profile decreases when the magnetic field parameter M become very large. Physically this is due to the effects of the transverse magnetic field on the conducting electrical fluid, which gives rise to a resistive type of Lorentz force that tends to slow down the fluid motion. Fig. 3 shows that a strong imposed magnetic force leads to a larger temperature. This is due to the fact that for strong magnetic force, the Lorenz force becomes dominant, and then the temperature of the liquid increases. Fig. 4 shows the effects of the mixed convection parameter λ on the velocity profile when $M, \beta_1, and\ Pr$ are fixed. It is worth noticing that by increasing the parameter λ reveals that buoyancy because of augments of gravity which boosts on the velocity $f'(\eta)$. Besides that, the thickness of boundary layer for large λ is also getting higher. In Fig. 5 we show that for larger λ, this would lead to increase in the temperature profile (this is much related to decrease in the boundary layer thickness). Fig. 6 is sketched for the variation of Prandtl number Pr on $\theta(\eta)$. It is noted that for lager Pr, the thermal field is lower and then this reduce the temperature.

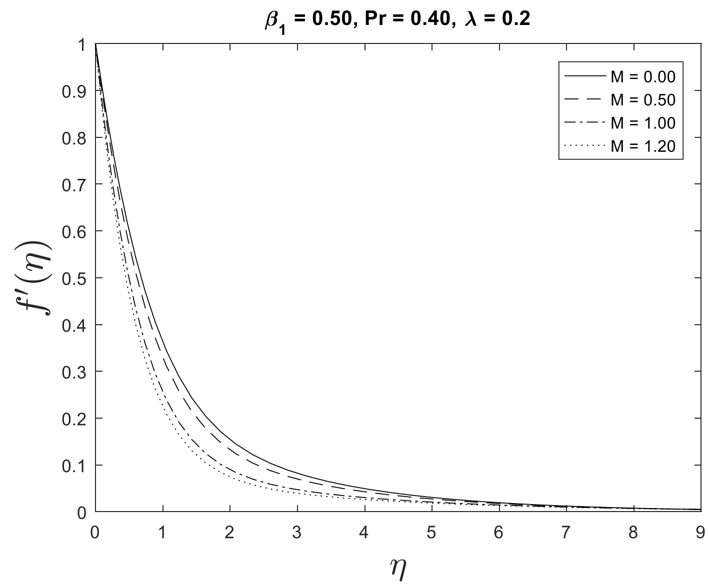

Fig. 2: Effects of Hartman number M for velocity$f'(\eta)$

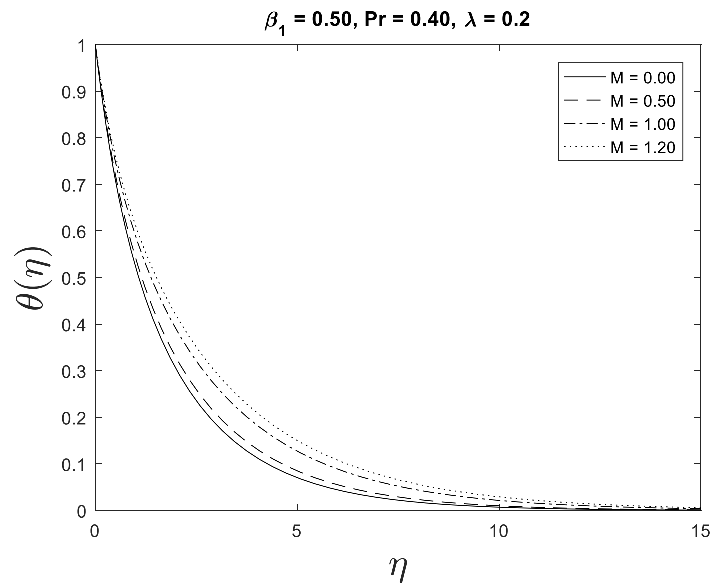

Fig. 3: Effects of Hartman number M for temperature $\theta(\eta)$

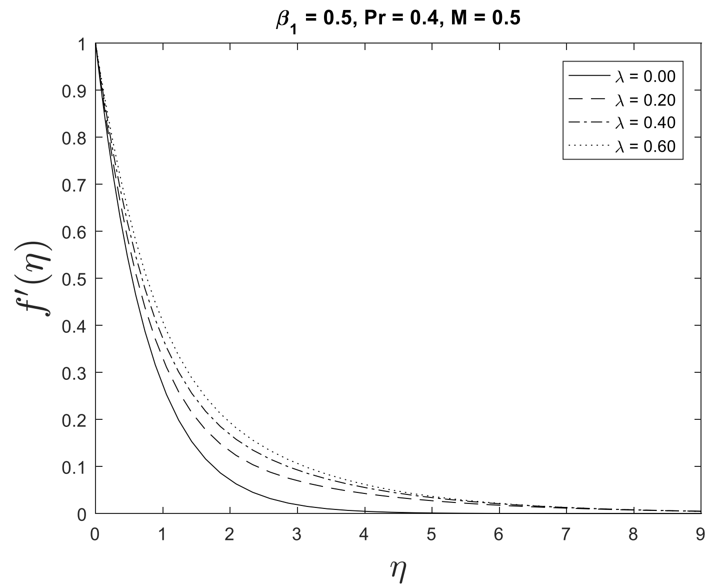

Fig. 4: Effects of mixed convection parameter λ for velocity $f'(\eta)$

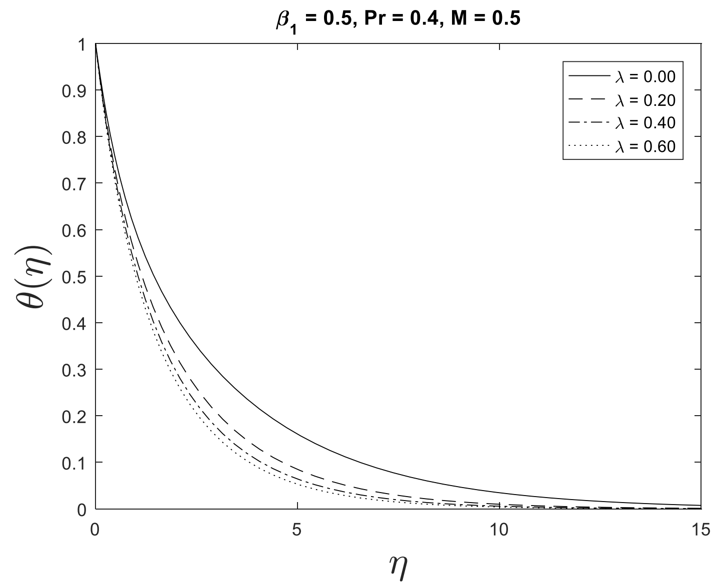

Fig. 5: Effects of mixed convection parameter λ for temperature $\theta(\eta)$

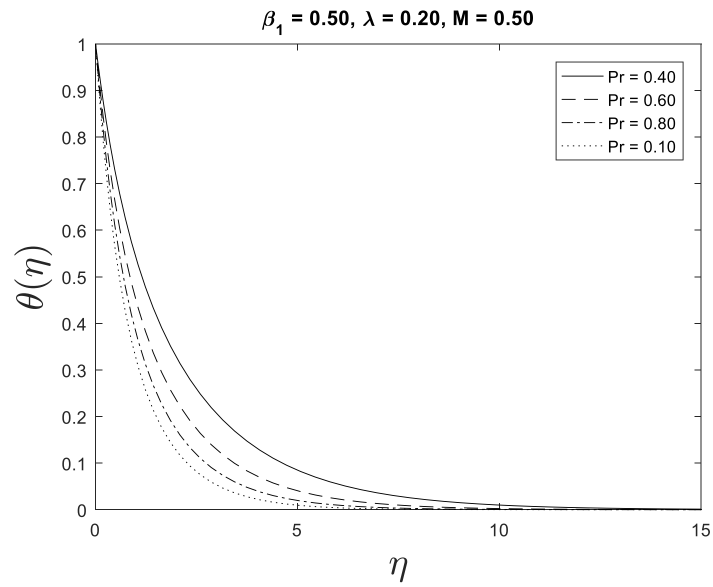

Fig. 6: Effects of Prandtl number Pr for temperature $\theta(\eta)$

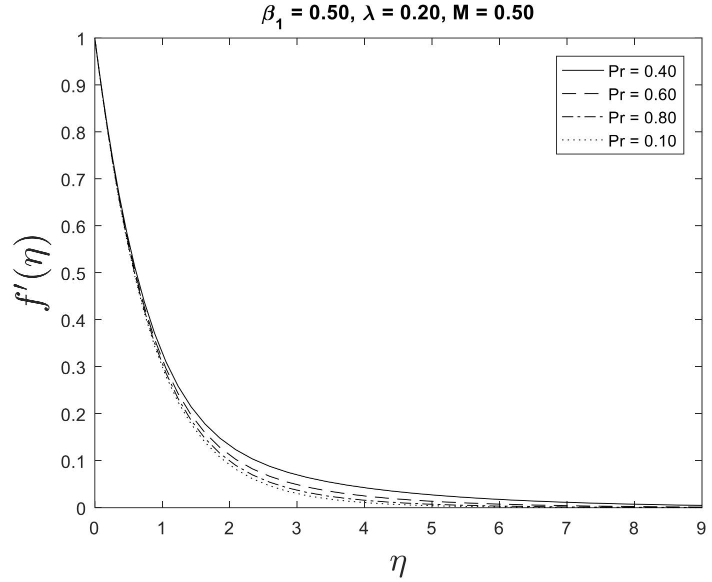

Fig. 7: Effects of Prandtl number Pr for velocity $f'(\eta)$

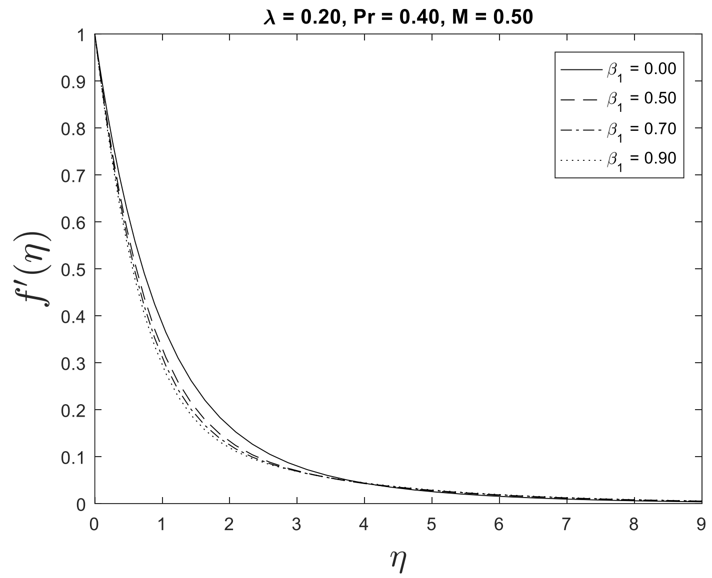

Fig. 8: Effects of Deborah number β_1 for velocity $f'(\eta)$

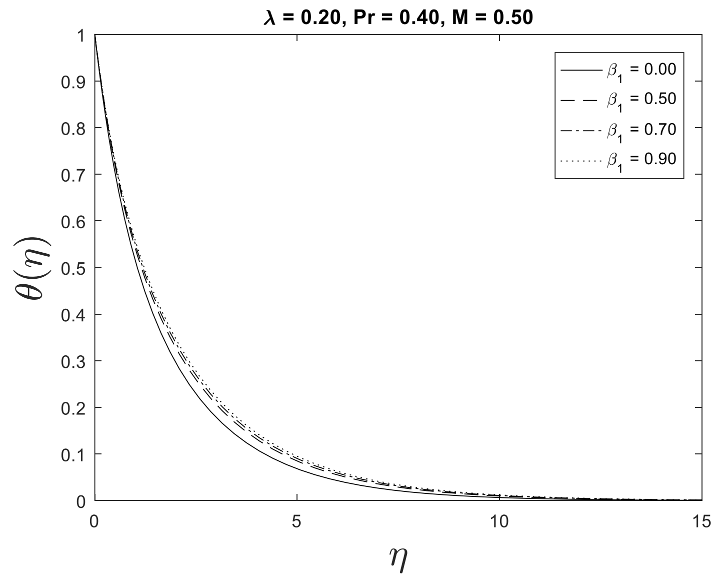

Fig. 9: Effects of Deborah number β_1 for temperature $\theta(\eta)$

In fact law Prandtl number Pr assist fluid with higher thermal conductivity and this create thicker thermal boundary layer than that for lager Pr. It is notice that from Fig. 7 Prandtl number Pr has same effect on $f'(\eta)$ same as temperature. The influence of Deborah number β_1 on the velocity distribution $f'(\eta)$ is shown through Fig. 8 and Fig. 9. In fact β_1 originally comes due to the relaxation time phenomena. There for large β_1 leads to longer relaxation time which opposes the fluid flow and then the thickness of momentum layer is reduced. Finally, Fig. 9 shows the effect of β_1 on temperature profile over the sheet, and we note that by increasing in β_1 parameter is seen to decrease and reducing in the liquid temperature $\theta(\eta)$. Physically, that is, for larger parameter β_1, the thermal boundary layer becomes thicker.

5. Conclusions

In this paper, the numerical solution to the MHD heat transfer problem of an incompressible Maxwell fluid over a stretched sheet channel has been obtained. SLM is knowledgeable in numerical solutions. The effects of various parameters are shown in several graphs. The validity of the current results was tested, and they were contrasted with those that had previously been published (Waqas et al., 2017; Megahed, 2013; Mukhopadhyay, 2012; Subhas Abel et al., 2012). Table 2 shows a limited example where there is strong agreement.

Compliance with ethical standards

Conflict of interest

The author(s) declared no potential conflicts of interest with respect to the research, authorship, and/or publication of this article.

References

Abdal S, Siddique I, Alrowaili D, Al-Mdallal Q, and Hussain S (2022). Exploring the magnetohydrodynamic stretched flow of Williamson Maxwell nanofluid through porous matrix over a permeated sheet with bioconvection and activation energy. Scientific Reports, 12: 278. https://doi.org/10.1038/s41598-021-04581-1 **PMid:34997184 PMCid:PMC8741956**

Ahmed MAM, Mohammed ME, and Khidir AA (2015). On linearization method to MHD boundary layer convective heat transfer with low pressure gradient. Propulsion and Power Research, 4(2): 105-113. https://doi.org/10.1016/j.jppr.2015.04.001

Aman S and Almdallal Q (2019). SA-copper based Maxwell nanofluid flow with second order slip effect using fractional derivatives. In the AIP Conference Proceedings, AIP Publishing, 2116: 030021. https://doi.org/10.1063/1.5114005

Aman S, Al-Mdallal Q, and Khan I (2020). Heat transfer and second order slip effect on MHD flow of fractional Maxwell fluid in a porous medium. Journal of King Saud University-Science, 32(1): 450-458. https://doi.org/10.1016/j.jksus.2018.07.007

Aman S, Khan I, Ismail Z, Salleh MZ, and Al-Mdallal QM (2017). Heat transfer enhancement in free convection flow of CNTs Maxwell nanofluids with four different types of molecular liquids. Scientific Reports, 7: 2445. https://doi.org/10.1038/s41598-017-01358-3 **PMid:28550289 PMCid:PMC5446429**

Cortell R (2006). A note on flow and heat transfer of a viscoelastic fluid over a stretching sheet. International Journal of Non-Linear Mechanics, 41(1): 78-85. https://doi.org/10.1016/j.ijnonlinmec.2005.04.008

Ellahi R, Hayat T, Javed T, and Asghar S (2008). On the analytic solution of nonlinear flow problem involving Oldroyd 8-constant fluid. Mathematical and Computer Modelling, 48(7-8): 1191-1200. https://doi.org/10.1016/j.mcm.2007.12.017

Esmaili Q, Ramiar A, Alizadeh E, and Ganji DD (2008). An approximation of the analytical solution of the Jeffery–Hamel flow by decomposition method. Physics Letters A, 372(19): 3434-3439. https://doi.org/10.1016/j.physleta.2008.02.006

Fetecau C, Prasad SC, and Rajagopal KR (2007). A note on the flow induced by a constantly accelerating plate in an Oldroyd-B fluid. Applied Mathematical Modelling, 31(4): 647-654. https://doi.org/10.1016/j.apm.2005.11.032

Ghadikolaei SS, Hosseinzadeh K, Yassari M, Sadeghi H, and Ganji DD (2018). Analytical and numerical solution of non-Newtonian second-grade fluid flow on a stretching sheet. Thermal Science and Engineering Progress, 5: 309-316. https://doi.org/10.1016/j.tsep.2017.12.010

Hayat T, Awais M, and Asghar S (2013). Radiative effects in a three-dimensional flow of MHD Eyring-Powell fluid. Journal of the Egyptian Mathematical Society, 21(3): 379-384. https://doi.org/10.1016/j.joems.2013.02.009

Hayat T, Khan M, and Ayub M (2004). Couette and Poiseuille flows of an Oldroyd 6-constant fluid with magnetic field. Journal of Mathematical Analysis and Applications, 298(1): 225-244. https://doi.org/10.1016/j.jmaa.2004.05.011

He JH (1999). Homotopy perturbation technique. Computer Methods in Applied Mechanics and Engineering, 178(3-4): 257-262. https://doi.org/10.1016/S0045-7825(99)00018-3

Husain M, Hayat T, Fetecau C, and Asghar S (2008). On accelerated flows of an Oldroyd-B fluid in a porous medium. Nonlinear Analysis: Real World Applications, 9(4): 1394-1408. https://doi.org/10.1016/j.nonrwa.2007.03.007

Hussain M, Hayat T, Asghar S, and Fetecau C (2010). Oscillatory flows of second grade fluid in a porous space. Nonlinear Analysis: Real World Applications, 11(4): 2403-2414. https://doi.org/10.1016/j.nonrwa.2009.07.016

Liao S (2004). On the Homotopy analysis method for nonlinear problems. Applied Mathematics and Computation, 147(2): 499-513. https://doi.org/10.1016/S0096-3003(02)00790-7

Liao SJ (1992). The proposed Homotopy analysis technique for the solution of nonlinear problems. Ph.D. Dissertation, Shanghai Jiao Tong University, Shanghai, China.

Makinde OD (2008). Effect of arbitrary magnetic Reynolds number on MHD flows in convergent-divergent channels. International Journal of Numerical Methods for Heat and Fluid Flow, 18(6): 697-707. https://doi.org/10.1108/09615530810885524

Makinde OD and Mhone PY (2006). Hermite–Padé approximation approach to MHD Jeffery–Hamel flows. Applied Mathematics and Computation, 181(2): 966-972. https://doi.org/10.1016/j.amc.2006.02.018

Makukula Z, Motsa SS, and Sibanda P (2010a). On a new solution for the viscoelastic squeezing flow between two parallel plates. Journal of Advanced Research in Applied Mathematics, 2(4): 31-38. https://doi.org/10.5373/jaram.455.060310

Makukula ZG, Sibanda P, and Motsa SS (2010b). A novel numerical technique for two-dimensional laminar flow between two moving porous walls. Mathematical Problems in Engineering, 2010: 528956. https://doi.org/10.1155/2010/528956

Malik MY, Hussain A, and Nadeem S (2013). Boundary layer flow of an Eyring–Powell model fluid due to a stretching cylinder with variable viscosity. Scientia Iranica, 20(2): 313-321.

Megahed AM (2013). Variable fluid properties and variable heat flux effects on the flow and heat transfer in a non-Newtonian Maxwell fluid over an unsteady stretching sheet with slip velocity. Chinese Physics B, 22(9): 094701. https://doi.org/10.1088/1674-1056/22/9/094701

Mukhopadhyay S (2012). Heat transfer analysis of the unsteady flow of a Maxwell fluid over a stretching surface in the presence of a heat source/sink. Chinese Physics Letters, 29(5): 054703. https://doi.org/10.1088/0256-307X/29/5/054703

Reddy NN, Rao VS, and Reddy BR (2021). Chemical reaction impact on MHD natural convection flow through porous medium past an exponentially stretching sheet in presence of heat source/sink and viscous dissipation. Case Studies in Thermal Engineering, 25: 100879. https://doi.org/10.1016/j.csite.2021.100879

Sadeghy K, Hajibeygi H, and Taghavi SM (2006). Stagnation-point flow of upper-convected Maxwell fluids. International Journal of Non-Linear Mechanics, 41(10): 1242-1247. https://doi.org/10.1016/j.ijnonlinmec.2006.08.005

Salah F, Abdul Aziz Z, and Chuan Ching DL (2011a). New exact solutions for MHD transient rotating flow of a second-grade fluid in a porous medium. Journal of Applied Mathematics, 2011: 823034. https://doi.org/10.1155/2011/823034

Salah F, Alzahrani AK, Sidahmed AO, and Viswanathan KK (2019). A note on thin-film flow of Eyring-Powell fluid on the vertically moving belt using successive linearization method. International Journal of Advanced and Applied Sciences, 6(2): 17-22. https://doi.org/10.21833/ijaas.2019.02.004

Salah F, Zainal AA, and Dennis LCC (2011b). Accelerated flows of a magnetohydrodynamic (MHD) second grade fluid over an oscillating plate in a porous medium and rotating frame. International Journal of Physical Sciences, 6(36): 8027-8035. https://doi.org/10.5897/IJPS11.1356

Saleem M, Al-Mdallal QM, Chaudhry QA, Noreen S, and Haider A (2020). Partial slip effects on the peristaltic motion of an upper-convected Maxwell fluid through an irregular channel. SN Applied Sciences, 2: 976. https://doi.org/10.1007/s42452-020-2457-1

Shafiq A, Çolak AB, and Naz Sindhu T (2021). Designing artificial neural network of nanoparticle diameter and solid–fluid interfacial layer on single-walled carbon nanotubes/ethylene glycol nanofluid flow on thin slendering needles. International Journal for Numerical Methods in Fluids, 93(12): 3384-3404. https://doi.org/10.1002/fld.5038

Shafiq A, Çolak AB, Sindhu TN, and Muhammad T (2022). Optimization of Darcy-Forchheimer squeezing flow in nonlinear stratified fluid under convective conditions with artificial neural network. Heat Transfer Research, 53(3): 67-89. https://doi.org/10.1615/HeatTransRes.2021041018

Shateyi S and Motsa SS (2010). Variable viscosity on magnetohydrodynamic fluid flow and heat transfer over an unsteady stretching surface with Hall effect. Boundary Value Problems, 2010: 257568. https://doi.org/10.1155/2010/257568

Si X, Li H, Zheng L, Shen Y, and Zhang X (2017). A mixed convection flow and heat transfer of pseudo-plastic power law nanofluids past a stretching vertical plate. International Journal of Heat and Mass Transfer, 105: 350-358. https://doi.org/10.1016/j.ijheatmasstransfer.2016.09.106

Subhas Abel M, Tawade JV, and Nandeppanavar MM (2012). MHD flow and heat transfer for the upper-convected Maxwell fluid over a stretching sheet. Meccanica, 47(2): 385-393. https://doi.org/10.1007/s11012-011-9448-7

Wang F, Ahmad S, Al Mdallal Q, Alammari M, Khan MN, and Rehman A (2022). Natural bio-convective flow of Maxwell nanofluid over an exponentially stretching surface with slip effect and convective boundary condition. Scientific Reports, 12: 2220. https://doi.org/10.1038/s41598-022-04948-y **PMid:35140256 PMCid:PMC8828818**

Waqas M, Khan MI, Hayat T, and Alsaedi A (2017). Stratified flow of an Oldroyd-B nanoliquid with heat generation. Results in Physics, 7: 2489-2496. https://doi.org/10.1016/j.rinp.2017.06.030

Xu YJ, Bilal M, Al-Mdallal Q, Khan MA, and Muhammad T (2021). Gyrotactic micro-organism flow of Maxwell nanofluid between two parallel plates. Scientific Reports, 11: 15142. https://doi.org/10.1038/s41598-021-94543-4 **PMid:34312440 PMCid:PMC8313715**

Zargartalebi H, Ghalambaz M, Noghrehabadi A, and Chamkha A (2015). Stagnation-point heat transfer of nanofluids toward stretching sheets with variable thermo-physical properties. Advanced Powder Technology, 26(3): 819-829. https://doi.org/10.1016/j.apt.2015.02.008